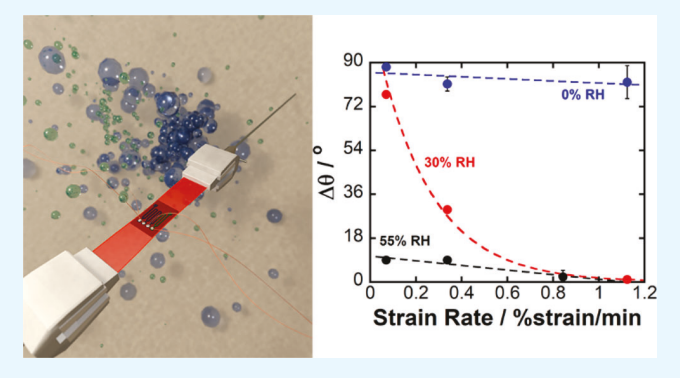


Humidity and Strain Rate Determine the Extent of Phase Shift in the Piezoresistive Response of PEDOT:PSS

Melda Sezen-Edmonds, † Vao-Wen Yeh, Nan Yao, and Yueh-Lin Loo*, †, \$ Dan Yao, and Yueh-Lin Loo*, † Nan Yao, †

Supporting Information

ABSTRACT: The piezoresistive response of PEDOT:PSS is sensitive to changes in its morphology when exposed to humidity and in response to different strain rates. The piezoresistive response of as-cast PEDOT:PSS transitions from being in-phase to being out-of-phase with applied strain when the relative humidity is reduced from >50% to near zero. At >50% relative humidity, the PSS matrix swells and interrupts the connectivity of electrically conducting PEDOT domains. Stretching PEDOT:PSS at such conditions leads to an increase in resistance with strain. Under dry conditions, PEDOT domains are connected; stretching PEDOT:PSS instead leads to preferential alignment of the conducting domains and a concomitant decrease in resistance. At



intermediate humidity, the piezoresistive response of PEDOT:PSS is phase shifted relative to applied strain, with it being out-of-phase at low strain rates (0.34%/min) and in-phase at high strain rates (1.12%/min). We interpret this peculiar and surprising observation as a competition between strain-induced domain separation and alignment, each having a different response time to applied strain. Postdeposition treatment of PEDOT:PSS with dichloroacetic acid removes excess PSS; PEDOT:PSS's piezoresistive response is then invariant with humidity and strain rate. Stabilizing its piezoresistive response can ensure accuracy of PEDOT:PSS-based flexible resistive sensors whose response to small strains is used to monitor environmental and human-health.

KEYWORDS: conducting polymers, PEDOT, humidity, strain, flexible electronics

1. INTRODUCTION

Poly(3,4-ethylenedioxythiophene):poly(styrenesulfonate), PE-DOT:PSS, is a water-dispersible and conducting polymer obtained through oxidative polymerization of 3,4-ethylenedioxythiophene, EDOT, along PSS. 1,2 In the last few decades since its discovery and commercialization, PEDOT:PSS has found uses in applications as wide ranging as electrodes and holetransport layers in solar cells and organic light-emitting diodes, 3,4 switchable active layers in electrochromic smart windows and displays, 5,6 as well as electrodes and sensing components in wearable electronics^{7,8} and bioelectronics.^{9,10} The ease in the processing and the mechanical compliance of PEDOT:PSS with flexible substrates have especially shown PEDOT:PSS to be suitable for flexible and conformable electronics. 11-13 The use of PEDOT:PSS in flexible and conformable electronics, however, requires an understanding of the impact of mechanical deformation on its electrical properties, or its piezoresistive response. 7,14,15

Piezoresistivity is defined as the change in the electrical resistance of conducting materials because of mechanical deformation, and this effect has previously been leveraged to monitor deformation and crack formation in civil structures, and human motion in medical applications. 16-18 The same piezoresistive effect, however, limits the use of conducting materials in flexible and conformable resistive sensor applications, as mechanical deformation, which is also transduced as part of the electrical signal, necessarily convolutes sensor readout.^{7,14} In a highly sensitive wearable thermoresistive sensor, for example, a 0.1% strain, which corresponds to the mechanical strain caused by breathing or pulsing of arteries, 19,20 can cause a 1 °C error in temperature reading.²¹ Given the fact that a few degrees increase in human body temperature indicates high fever, this temperature error that occurs under small strains due to normal human activity prevents these sensors from being broadly deployed as wearable sensors. In this work, we focus on understanding the robustness of the piezoresistive response of PEDOT:PSS in

Received: January 14, 2019 Accepted: April 16, 2019 Published: April 16, 2019

[†]Department of Chemical and Biological Engineering, Princeton University, Princeton, New Jersey 08544, United States [‡]Princeton Institute for Science and Technology of Materials, Princeton University, Princeton, New Jersey 08544, United States

[§]Andlinger Center for Energy and the Environment, Princeton University, Princeton, New Jersey 08544, United States

these subtle deformation regimes (<0.3% strain) for wearable sensor or environmental health monitoring applications.

Subjecting PEDOT:PSS to mechanical deformation can cause an increase in its resistance (resistance change is in-phase with strain), which may stem from increased separation between conducting domains on strain.²² Alternatively, one may observe a decrease in resistance (resistance change is outof-phase with strain), which has been attributed to straininduced alignment or coalescence of conducting domains.²³ Our previous studies on another conducting polymer complex, polyaniline-poly(2-acrylamido-2-methyl-1-propanesulfonic acid), PANI-PAAMPSA, have shown the polarity of its piezoresistive response to be dependent on its thin-film morphology that can be prescribed, either at the onset of synthesis, or through postdeposition processing. 7,22 PANI-PAAMPSA films that exhibit high crystallinity and whose conducting domains are interconnected show a resistance response that is out-of-phase with applied strain, whereas PANI-PAAMPSA films that are less crystalline exhibit a resistance response that is in-phase with applied strain. In both cases, the change in the resistance with strain is linear in the strain range tested. Interestingly, the piezoresistive response of as-cast PEDOT:PSS films deviates from this linearity and is further phase-shifted (not fully in-phase or out-of-phase) with respect to applied strain. While this phenomenon has important implications on the utility of PEDOT:PSS and its robustness and reliability as sensors, the source of this peculiar piezoresistive response was unknown.⁷

Herein, we report experimental results that implicate the morphology of PEDOT:PSS to be responsible of this deviation from linearity in the piezoresistive response of as-cast PEDOT:PSS and show that the extent of phase shift depends both on the rate at which the films are deformed, and on the relative humidity. Unlike PANI-PAAMPSA, which shows strain-rate and humidity independent piezoresistive response, 7,24 PEDOT:PSS can exhibit either completely inphase, completely out-of-phase, or phase-shifted piezoresistive response in a single sample, accessible by changing the ambient relative humidity and/or the strain rate. We correlate the humidity-dependent changes in the piezoresistive response of PEDOT:PSS with the morphological changes caused by water absorption by hygroscopic PSS. Given the coupled effect of strain rate and humidity on the piezoresistive response of ascast PEDOT:PSS, a simple normalization to account for both effects is not always possible for ensuring the accuracy of flexible sensors and bioelectronic devices. A workaround to this coupled effect and to deconvolute the pressure and humidity responses, PEDOT:PSS-based sensors that are deposited on quartz crystal microbalance and incorporate complex neural network algorithms have been previously developed.²⁵ Here, we present our understanding of the sources of this coupled effect, and propose exposing PEDOT:PSS to dichloroacetic acid, DCA, to reduce its sensitivity toward humidity and strain rate. DCA treatment is known to enhance the electrical conductivity of PEDOT:PSS through structural modification and removal of excess PSS.³ Herein, we show that the DCA-treatment induced morphological change also enhances the robustness of the piezoresistive response of PEDOT:PSS films, making them resistant to changes in the ambient humidity and strain rate.

2. RESULTS AND DISCUSSION

Figure 1a shows the change in resistance of as-cast PEDOT:PSS (Clevios P, Heraeus) patterns under cyclic strain

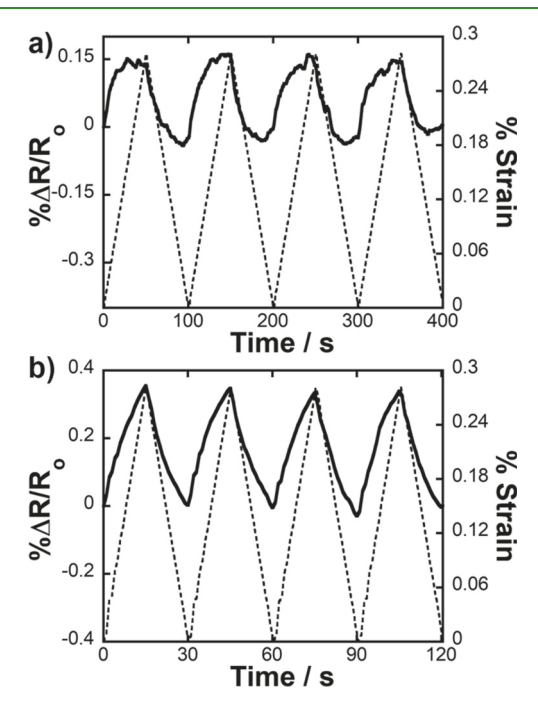


Figure 1. Relative change in resistance of as-cast Clevios P patterns (solid line) under cyclic strain (dashed line) applied at (a) 0.34% strain/min and (b) 1.12% strain/min. All tests were performed at ambient conditions in 55% relative humidity.

at a rate of 0.34% strain/min in air (55% relative humidity). We chose to focus on small strains, as these strain levels are relevant for many applications, including strain gauges for monitoring building health, and wearable sensors for monitoring the arterial pulse and breathing. 19,26 When the PEDOT:PSS pattern is stretched, its resistance increases with strain; the resistance recovers to its original value when the strain is released as shown in Figure 1a. The resistance, however, does not change linearly with applied strain; it instead plateaus ahead of the applied strain on loading and unloading. This plateauing is rather unusual since we performed the tests in the elastic regime of PEDOT:PSS.^{27,28} The resistance response curve of PEDOT:PSS patterns is also not completely in-phase with the applied strain. To quantify this deviation in resistance response, we calculated the phase difference between the resistance change and applied strain $(\Delta\theta)$. A $\Delta\theta$ of 90° specifies that the resistance is completely out-of-phase with applied strain; a $\Delta\theta$ of 0° specifies that the resistance is in-phase with applied strain. The PEDOT:PSS pattern exhibits a $\Delta \theta$ of about 9° when tested in air at an applied strain rate of 0.34% strain/min.

To further investigate the source of this phase shift in the piezoresistive response of PEDOT:PSS patterns, we varied the strain rate while keeping the magnitude of the maximum applied strain and all other conditions the same. Figure 1b shows the change in resistance of the PEDOT:PSS pattern when a cyclic strain rate of 1.12% strain/min instead of 0.34% strain/min is applied. When tested at this higher strain rate, $\Delta\theta$ is almost zero, and the resistance response of PEDOT:PSS patterns increases and decreases more linearly on loading and

ACS Applied Materials & Interfaces

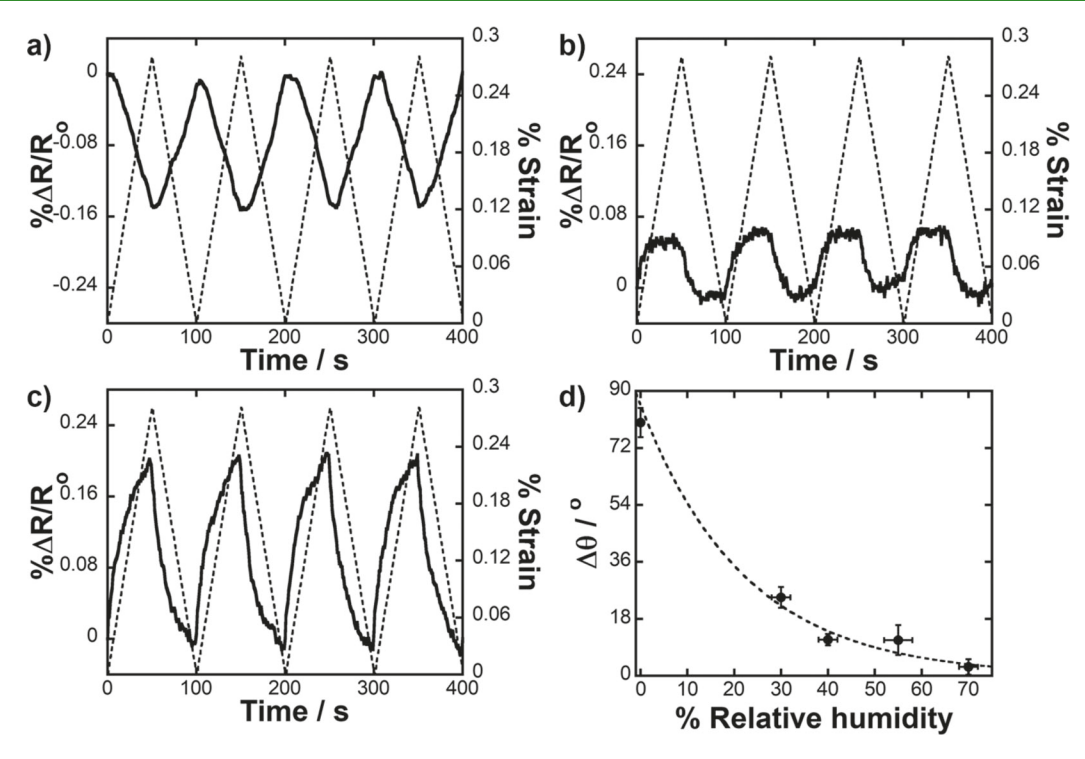


Figure 2. Relative change in resistance of as-cast Clevios P patterns (solid line) under cyclic strain (dashed line) at (a) 0%, (b) 30%, and (c) 70% relative humidity. (d) Phase difference between resistance response and applied strain ($\Delta\theta$) with varying relative humidity. Cyclic strain is applied at a rate of 0.34% strain/min.

unloading, respectively. When the strain rate is lowered to 0.07% strain/min, however, the PEDOT:PSS pattern loses its sensitivity to applied strain and the resistance change becomes indifferentiable from noise. This dependence of $\Delta\theta$ with strain rate is reversible and independent of the order with which these strain rates are imposed on the samples.

Such nonlinearity in the piezoresistive response with strain or strain rate has previously been observed in composite materials and has been attributed to the presence of multiple components, each having a different response time to the applied strain.²⁹⁻³³ In carbon nanotube composites, for example, the contact distance between individual nanotubes can change with applied strain, which can impact the alignment or conformation of individual nanotubes, as well as the percolation of nanotubes within the insulating polymer matrix. 17,29,34,35 Each of these phenomena contributes to the aggregate piezoresistive response of the composite with a different time constant and to a different extent, the combination of which manifests a strain-rate dependent piezoresistive response. 32 In a similar vein, PEDOT:PSS thin films are structurally and compositionally heterogeneous; we therefore speculate that its piezoresistive response likely reflects the compound effects of strain on its structuring at different length scales. In particular, PEDOT:PSS thin films comprise conducting PEDOT:PSS domains that have a PEDOT-rich interior and a PSS-rich exterior; these domains are dispersed in an insulating PSS matrix.³⁶⁻³⁸ We therefore believe the strain-rate dependence piezoresistive response to stem from the structural and compositional heterogeneities of PEDOT:PSS thin films, and in particular how deformation impacts the connectivity of conducting PEDOT-rich domains at different strain rates.

It follows that any external parameter that influences the spatial distribution of PEDOT-rich domains will likely impact its piezoresistive response and its strain-rate dependence. And given the hygroscopicity of PSS, water uptake, which has been reported to cause substantial swelling of PSS-rich domains and alter the distribution and connectivity of electrically conducting domains in PEDOT:PSS thin films, impacts both the electrical conductivity and mechanical properties of PEDOT:PSS. Water uptake should thus be a tuning parameter with which we see differences in the piezoresistive response and its strain-rate dependence in PEDOT:PSS.

To verify, we performed strain tests on PEDOT:PSS patterns as a function of humidity. We accessed near-zero relative humidity by keeping PEDOT:PSS patterns under vacuum for at least 3 h and encapsulating the dried films in a N₂-filled glovebox prior to testing. Figure 2a shows the change in resistance of PEDOT:PSS patterns under cyclic strain applied at 0.34% strain/min at 0% relative humidity. The resistance of PEDOT:PSS patterns is always out-of-phase ($\Delta\theta$ = $80 \pm 4.6^{\circ}$) with applied strain when tested at 0% relative humidity. This out-of-phase behavior is preserved even at the highest strain rate (1.12% strain/min), as seen in Figure 3 (blue circles). Seeing this dramatic change in the piezoresistivity response of PEDOT:PSS in the absence of humidity, we conducted additional experiments at varying relative humidities. Figures 2b and c show the piezoresistive responses of PEDOT:PSS patterns at 30% and 70% relative humidities, respectively, tested at a fixed strain rate of 0.34% strain/min. Figure 2d summarizes how $\Delta\theta$ varies with relative humidity for PEDOT:PSS patterns tested at this fixed strain rate. As the humidity increases from 0% to 70%, $\Delta\theta$ gradually switches from 90° to 0°. At 30% relative humidity, $\Delta\theta$ of PEDOT:PSS patterns is $24.8 \pm 3.3^{\circ}$; this phase shift is almost three times that observed in air (55% relative humidity) at the same strain rate.

ACS Applied Materials & Interfaces

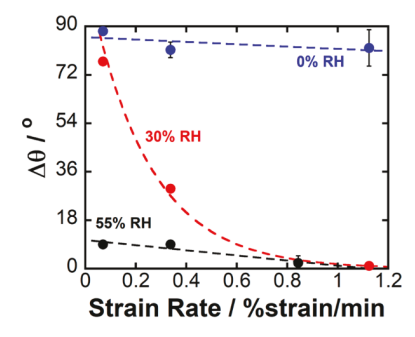


Figure 3. Phase difference between resistance and applied strain under varying strain rate for as-cast Clevios P patterns at 55% (black), 30% (red), and 0% (blue) relative humidity.

Per our earlier hypothesis, we interpret the progressive change in $\Delta\theta$ from 90° to 0° with increasing humidity to reflect changes in morphology. Specifically, water absorption causes swelling of the PSS shell and matrix, which is reported to increase the separation between conducting PEDOT-rich domains.36,39 This swollen-PSS shell and matrix disrupts the connectivity between conducting domains. Imposing tensile strain on such films is expected to further increase the separation between conducting domains, which manifests a positive change in resistance with applied strain. At low humidities, there is less swelling of PSS. The conducting domains thus remain connected and the PEDOT-rich core from neighboring particles can interact with each other. 27,40 Tensile deformation is likely to improve alignment of conducting PEDOT segments in these connected conducting domains. This improved alignment can in turn promote charge transport, resulting in a decrease in the overall resistance of PEDOT:PSS patterns on applied strain. Depending on the details of morphology, which depends on water absorption, the competition between increased particle separation and improved PEDOT alignment determines the composite piezoresistive response of PEDOT:PSS.

Humidity also significantly impacts the extent of strain-rate dependence of the piezoresistive response of PEDOT:PSS, as shown in Figure 3. At 0% relative humidity, we access a $\Delta\theta$ of 90° that is independent of strain rate, likely because the conducting domains are well connected in the absence of water. With these domains connected, their alignment dominates piezoresistive response. On the other hand, at 70% relative humidity, $\Delta\theta$ of PEDOT:PSS patterns is 0° and its piezoresistive response, too, is independent of strain rate. We take this observation to imply that swelling of PSS-rich regions prevents neighboring PEDOT-rich domains from interacting with each other at these high relative humidities, with separation between conducting domains now dominating the piezoresistive response at all strain rates. When tested at intermediate relative humidities, the extent of phase shift in the piezoresistive response of PEDOT:PSS is strain-rate dependent (Figure 3, red circles). When PEDOT:PSS patterns are tested at 30% relative humidity, for example, $\Delta\theta$ approaches 90° when the applied strain rate is decreased to 0.07% strain/ min (Figure S1a). When the strain rate is increased to 1.12% strain/min at the same relative humidity of 30%, on the other hand, $\Delta\theta$ approaches 0° (Figure S1b). We believe that, at this intermediate relative humidity, at which PSS-rich regions are partially swollen, the mechanism by which PEDOT:PSS responds to applied strain is now strain-rate dependent given each mechanism is expected to have different response time to

applied strain. Our piezoresistivity measurements implicate that, at lower strain rates, improved domain alignment dominates whereas at higher strain rates, domain separation dominates. Compiling the piezoresistive response of PEDOT:PSS across the different strain rates and relative humidities, we see that the resistive response generally becomes more in-phase with increasing strain rates, and with increasing humidity.

Given these observations, we further hypothesize that reducing the hygroscopic PSS content that separates conducting domains should improve the connectivity of conducting domains and eliminate this humidity and strainrate dependence. We previously reported that polyaniline that is template polymerized on poly(2-acrylamido-2methyl-1propanesulfonic acid), PANI-PAAMPSA, does not exhibit strain rate or humidity dependence in its piezoresistive response despite having a hygroscopic polymer-acid template that is similar to that in PEDOT:PSS.^{7,24} We attributed this invariance in PANI-PAAMPSA's piezoresistive response to the robustness of its solid-state morphology with conducting PANI domains surrounding the hygroscopic PAAMPSA-rich regions.²⁴ To test our hypothesis that humidity and strain-rate dependence of the piezoresistivity of PEDOT:PSS arises due to having excess free PSS between its conducting domains, we solvent annealed PEDOT:PSS patterns in dichloroacetic acid, DCA. Exposing PEDOT:PSS thin films to solvents, such as DCA, is known to remove excess free PSS as evidenced by Xray photoelectron spectroscopy studies and improve the connectivity of the conducting PEDOT domains. 3,37 Reflectivity measurements performed by Bießmann et al. supports our hypothesis that such post-treatment morphological changes reduce water-absorption induced swelling of PE-DOT:PSS films. 41 Figure 4 shows the dependence of $\Delta\theta$ on

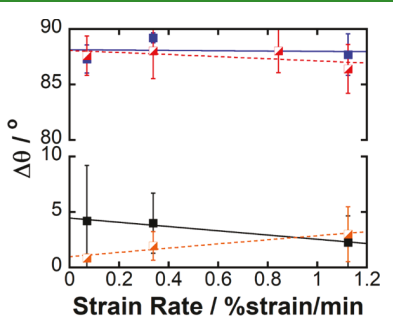


Figure 4. Phase difference between resistance response and applied strain $(\Delta\theta)$ at varying strain rate for DCA-treated Clevios P pattern at 55% (black) and 0% (orange) relative humidity and DCA-treated Clevios PH 1000 pattern at 55% (blue) and 0% (red) relative humidity. Y-axis break between 10° and 80° is used for better visualization of the error bars and shows $\Delta\theta$ is almost constant with strain rate.

applied strain rate for DCA-treated PEDOT:PSS patterns tested both at 0% and 55% relative humidity (orange and black rectangles; see Figures S2 for the cyclic piezoresistive response curves of DCA-treated PEDOT:PSS patterns). The $\Delta\theta$ of DCA-treated patterns is invariant ($\Delta\theta<5^\circ$) with humidity and strain rate, unlike the $\Delta\theta$ of as-cast PEDOT:PSS patterns, which spans the full range of 90° with humidity and/or strain rate (Figure 3). This observation is consistent with our hypothesis that reducing PSS content improves connectivity between PEDOT-rich domains, and enhances the

stability of the piezoresistive response of PEDOT:PSS patterns under varying humidity and strain rate.

To assess the generalizability of our findings, we also tested the strain-rate and the humidity dependence of the piezoresistive response of a commonly used, high conductivity grade of PEDOT:PSS, Clevios PH 1000 (Heraeus). Figure S3 shows that Clevios PH 1000 patterns also show strain-rate dependent piezoresistive responses when tested in air, with $\Delta\theta$ approaching zero as the strain rate is increased. At 0% relative humidity, the piezoresistive response of Clevios PH 1000 is strain-rate independent, as seen in Figure S4, and a $\Delta\theta$ of 90° is accessed at all strain rates (Figure S3d, triangles), similar to what we observe for the Clevios P patterns (Figure 3, red circles). Upon exposure to DCA, the piezoresistive response of Clevios PH 1000 is also stabilized, and we eliminate the phaseshift in the piezoresistive response with strain rate and humidity, as seen in Figure 4 (red and blue rectangles; see Figure S5 for cyclic piezoresistive response curves).

Unexpectedly, Clevios PH 1000 patterns consistently have a $\Delta\theta$ of 90° after DCA treatment while Clevios P patterns consistently have a $\Delta\theta$ of 0° (<5° as seen in Figure 4). Following the rationale that the piezoresistive response in PEDOT:PSS is morphology dependent, we surmise this difference must stem from differences in morphology that arises on DCA treatment. While directly visualizing the morphological changes with strain rate and humidity is challenging given the small strains under which the experiments take place, we have been able to image these films after DCA treatment that support our assertion. Figure 5 contains

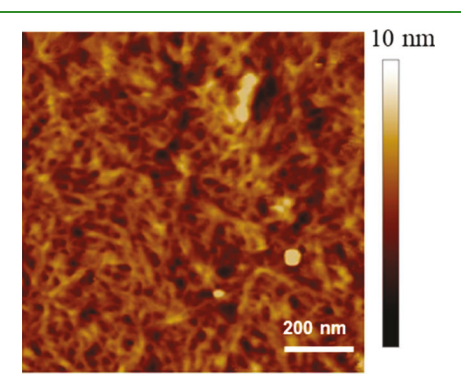


Figure 5. AFM image of DCA-treated Clevios PH 1000 film showing the mesh of fibrillar domains.

an atomic force microscopy (AFM) image of a DCA-treated Clevios PH 1000 film that reveals an interconnected mesh of

fiber-like structures. The presence of such fibrillar domains with comparable dimensions was previously observed by Kim et al. through high-angle annular dark-field scanning transmission electron microscopy (HAADF STEM) experiments. 42 We speculate that stretching DCA-treated Clevios PH 1000 films possessing such fibrillar networks improves their alignment in a manner similar to what had been observed in graphene- or carbon nanotube-coated fabrics or yarns. 43,44 This alignment in turn results in a decrease in resistance ($\Delta\theta$ of 90°). HAADF STEM images of as-cast and DCA-treated Clevios P films are shown in Figure 6a and b. After DCA treatment, we observe instead bright white isolated spots (Figure 6b), which have been confirmed to be PEDOT crystallites via STEM electron diffraction (Figure 6c). Different from the mesh-like fibrillar networks seen in DCA-treated Clevios PH 1000 films, these PEDOT crystallites are individually isolated. Stretching DCA-treated Clevios P patterns is likely to further separate the PEDOT crystallites and result in an increase in resistance ($\Delta\theta$ of 0°). Altogether, our findings implicate that subtle changes in morphology impose big differences in the piezoresistive response of PEDOT:PSS.

3. CONCLUSION

The piezoresistive response of as-cast PEDOT:PSS is humidity and strain-rate dependent. Water absorption from air by hygroscopic PSS swells the PSS-rich regions that separate conducting PEDOT-rich regions. This swelling in turn affects the piezoresistive response of PEDOT:PSS. At intermediate extents of swelling, the piezoresistive response of PEDOT:PSS is strain-rate dependent; we interpret this observation as a competition between the relative dominance of strain-induced domain separation and improved domain connectivity, each having a different response time to applied strain. Although further studies are needed to quantify the time scales with which different morphological features in PEDOT:PSS respond to mechanical deformation, the results from our study reminds us of the concept of time-temperature superposition in polymer viscoelasticity. Specifically, our piezoresistive characterization suggests that, at a given humidity, or equivalently for a given morphology, lower strain rates should favor the alignment of conducting domains by providing sufficient time for structural rearrangement. When PEDOT:PSS films are stretched rapidly, on the other hand, there is insufficient time for the conducting domains to interact with each other, so separation of conducting domains dominate the piezoresistive response of PEDOT:PSS. The

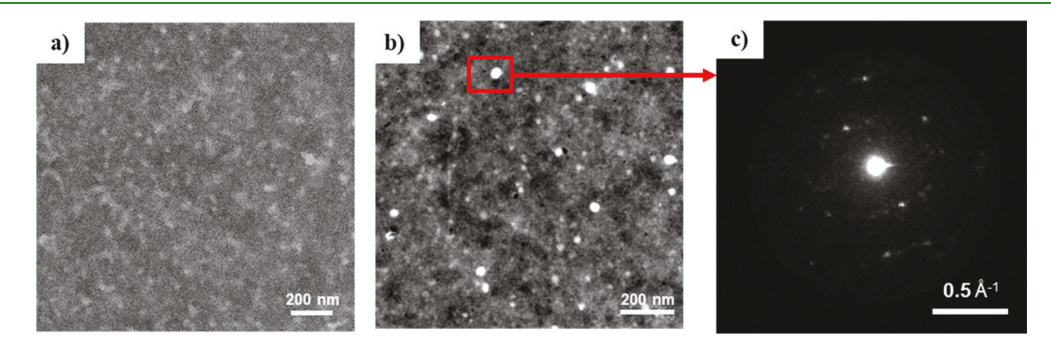


Figure 6. HAADF STEM images of (a) as-cast and (b) DCA-treated Clevios P films. (c) Diffraction pattern obtained from the highlighted spot in panel b.

interdependence of humidity and strain rate must be considered when incorporating pristine PEDOT:PSS into flexible electronics as sensing elements. By employing postdeposition solvent annealing that removes excess PSS, we can access completely in-phase or completely out-of-phase resistance response curves in PEDOT:PSS patterns, independent of applied strain rate and humidity. This increased stability can ensure the accuracy of flexible PEDOT:PSS-based humidity and chemical sensors both for environmental and human-health monitoring applications.

4. EXPERIMENTAL SECTION

4.1. Preparation of PEDOT:PSS Patterns on Polyimide. We prepared serpentine patterns of different grades of PEDOT:PSS (Clevios P or Clevios PH 1000, Heraeus, PEDOT:PSS ratio 1:2.5 w/ w) on polyimide (5 mil Kapton, Fralock) substrates, as described in our previous work, to evaluate their piezoresistive response. Serpentine patterns were used to maximize the effective length of the conducting polymer in one direction and minimize it in the transverse direction. Straining along the long axis of these patterns minimizes traverse strain effects in our measurements. DCA treatment was performed by vigorously shaking the PEDOT:PSS-patterned polyimide in 100 °C DCA for 3 min, as described by Yoo et al.³ The samples are then baked at 140 °C for 30 min and kept under vacuum for at least 3 h prior to testing. The thicknesses of the serpentine patterns were approximately 500 nm. Encapsulation was performed by gluing another piece of polyimide on PEDOT:PSS-patterned polyimide using Araldite 2000+. During the encapsulation process, it was ensured that Araldite 2000+ does not touch the PEDOT:PSS

4.2. Strain Tests. We performed cyclic strain tests in the elastic deformation regime (<2% strain)²⁷ of PEDOT:PSS patterns by uniaxially stretching the patterns in their strain sensitive direction using an Instron electromechanical universal testing machine (model 5969).7 Four equally spaced copper wires were attached to PEDOT:PSS patterns as contacts, and the resistances of the samples were recorded during the strain tests using a four-probe geometry with Agilent 4145B Semiconductor Parameter Analyzer. After performing the strain tests in air (55 \pm 3% relative humidity), the samples were kept under vacuum for at least 3 h and encapsulated in a N₂-filled glovebox for testing at a 0% relative humidity condition. For testing at 70 \pm 2% and 30 \pm 2% relative humidities, samples were kept at the respective humidities, by exposure to the atmosphere of a saturated NaCl salt bath, and/or with desiccant overnight. The humidities were monitored with a humidity sensor and PEDOT:PSS samples were only exposed to the corresponding relative humidity after the atmosphere has stabilized. The samples were then encapsulated in the humidity chamber before taken out for strain testing. To ensure that the encapsulation process does not alter the strain tests, we opened a window on the encapsulating polyimide layer at the end of the humidity tests, and exposed PEDOT:PSS films to air again without fully removing the encapsulation layer. We were able to reproduce the initial results obtained when the films were tested in air prior to encapsulation.

For quantifying the phase shift between resistance and strain, we assumed that at applied strain is zero at 0° and is maximum at 90°. The phase shift corresponds to the difference in the angle at which the minima or the maxima of resistance and applied strain were observed.

4.3. Characterization. For AFM experiments, as-purchased PEDOT:PSS dispersions (Clevios PH 1000, Heraeus) were spin coated on precleaned glass substrate at 1000 rpm for 60 s. Films were then dried at $100\,^{\circ}\text{C}$ for 5 min. DCA treatment was performed as described above. These samples were processed in manners identical to those used to fabricate the serpentine patterns.

AFM images were collected in tapping mode with Veeco Dimensions Nanoman. Antimony-doped silicon AFM tips with a spring constant of 40 N m⁻¹ (Bruker, model MPP-11100-10) were

used. Image analysis was performed using NanoScope analysis software.

HAADF images of PEDOT:PSS thin films were acquired using Talos F200X STEM. Pelco silicon aperture frames without support film (0.1 mm × 0.1 mm windows; Ted Pella, Inc.) were used as TEM grids. Photoresist (AZ 1518; MicroChemicals GmbH) was spin coated on precleaned glass substrates at 4000 rpm for 40 s as a sacrificial layer and was annealed at 90 °C for 1 min. The photoresist layer was then exposed to oxygen plasma for 10 s to increase its hydrophilicity. As-purchased PEDOT:PSS (Clevios P, Heraeus) was spin coated at 5000 rpm for 40 s on this photoresist-coated glass, and annealed at 140 °C for 5 min. With a razor blade, approximately 4 mm × 4 mm squares were scored, and the substrate was slowly immersed in acetone. As acetone dissolves the photoresist layer, PEDOT:PSS squares float to the surface of acetone. Free-standing PEDOT:PSS films were then picked up with the TEM grids. The films were dried at 100 °C for 5 min. DCA treatment was performed by keeping PEDOT:PSS-coated TEM grids in 100 $^{\circ}\text{C}$ DCA for 10 min, and annealing at 140 °C for 30 min. All samples were kept under vacuum overnight before testing. PEDOT:PSS-coated TEM grids were loaded onto a Talos F200x STEM that is operated at an accelerating voltage of 200 kV. HAADF STEM images were collected at room temperature at below 10⁻⁷ Torr pressure.

ASSOCIATED CONTENT

S Supporting Information

The Supporting Information is available free of charge on the ACS Publications website at DOI: 10.1021/acsami.9b00817.

Relative change in resistance of Clevios P and PH 100 patterns (PDF)

AUTHOR INFORMATION

Corresponding Author

*E-mail: lloo@princeton.edu.

ORCID ®

Melda Sezen-Edmonds: 0000-0003-0476-6815

Yueh-Lin Loo: 0000-0002-4284-0847

Author Contributions

The manuscript was written through contributions of all authors. All authors have given approval to the final version of the manuscript.

Notes

The authors declare no competing financial interest.

ACKNOWLEDGMENTS

This work was partially supported by the Anonymous Fund, sponsored by the School of Engineering and Applied Science at Princeton University and by Princeton Center for Complex Materials that was funded by NSF-MRSEC under NSF award DMR-1420541 and an NSF grant to Y.L.L. (CMMI-1824674). The authors acknowledge Prof. Craig B. Arnold for access to the Instron.

REFERENCES

- (1) Heywang, G.; Jonas, F. Poly(Alkylenedioxythiophene)s New, Very Stable Conducting Polymers. *Adv. Mater.* **1992**, *4*, 116–118.
- (2) Elschner, A.; Kirchmeyer, S.; Lovenich, W.; Merker, U.; Reuter, K. PEDOT: Principles and Applications of an Intrinsically Conductive Polymer; CRC Press, 2010; p 145.
- (3) Yoo, J. E.; Lee, K. S.; Garcia, A.; Tarver, J.; Gomez, E. D.; Baldwin, K.; Sun, Y.; Meng, H.; Nguyen, T.-Q.; Loo, Y.-L. Directly Patternable, Highly Conducting Polymers for Broad Applications in Organic Electronics. *Proc. Natl. Acad. Sci. U. S. A.* **2010**, *107*, 5712–5717.

- (4) Fehse, K.; Walzer, K.; Leo, K.; Lövenich, W.; Elschner, A. Highly Conductive Polymer Anodes as Replacements for Inorganic Materials in High-Efficiency Organic Light-Emitting Diodes. *Adv. Mater.* **2007**, *19*, 441–444.
- (5) Davy, N. C.; Sezen-Edmonds, M.; Gao, J.; Lin, X.; Liu, A.; Yao, N.; Kahn, A.; Loo, Y.-L. Pairing of Near-Ultraviolet Solar Cells with Electrochromic Windows for Smart Management of the Solar Spectrum. *Nat. Energy* **2017**, *2*, 17104.
- (6) Beni, V.; Nilsson, D.; Arven, P.; Norberg, P.; Gustafsson, G.; Turner, A. P. F. Printed Electrochemical Instruments for Biosensors. *ECS J. Solid State Sci. Technol.* **2015**, *4*, S3001–S3005.
- (7) Sezen, M.; Register, J. T.; Yao, Y.; Glisic, B.; Loo, Y.-L. Eliminating Piezoresistivity in Flexible Conducting Polymers for Accurate Temperature Sensing under Dynamic Mechanical Deformations. *Small* **2016**, *12*, 2832–2838.
- (8) Savagatrup, S.; Chan, E.; Renteria-Garcia, S. M.; Printz, A. D.; Zaretski, A. V.; O'Connor, T. F.; Rodriquez, D.; Valle, E.; Lipomi, D. J. Plasticization of PEDOT:PSS by Common Additives for Mechanically Robust Organic Solar Cells and Wearable Sensors. *Adv. Funct. Mater.* **2015**, *25*, 427–436.
- (9) Jonsson, A.; Inal, S.; Uguz, I.; Williamson, A. J.; Kergoat, L.; Rivnay, J.; Khodagholy, D.; Berggren, M.; Bernard, C.; Malliaras, G. G.; Simon, D. T. Bioelectronic Neural Pixel: Chemical Stimulation and Electrical Sensing at the Same Site. *Proc. Natl. Acad. Sci. U. S. A.* **2016**, *113*, 9440–9445.
- (10) Isaksson, J.; Kjäll, P.; Nilsson, D.; Robinson, N. D.; Berggren, M.; Richter-Dahlfors, A. Electronic Control of Ca²⁺ Signalling in Neuronal Cells Using an Organic Electronic Ion Pump. *Nat. Mater.* **2007**, *6*, 673–679.
- (11) Khodagholy, D.; Doublet, T.; Gurfinkel, M.; Quilichini, P.; Ismailova, E.; Leleux, P.; Herve, T.; Sanaur, S.; Bernard, C.; Malliaras, G. G. Highly Conformable Conducting Polymer Electrodes for in Vivo Recordings. *Adv. Mater.* **2011**, *23*, 268–272.
- (12) Vijay, V.; Rao, A. D.; Narayan, K. S. In Situ Studies of Strain Dependent Transport Properties of Conducting Polymers on Elastomeric Substrates. *J. Appl. Phys.* **2011**, *109*, 084525.
- (13) Lipomi, D. J.; Chong, H.; Vosgueritchian, M.; Mei, J.; Bao, Z. Toward Mechanically Robust and Intrinsically Stretchable Organic Solar Cells: Evolution of Photovoltaic Properties with Tensile Strain. *Sol. Energy Mater. Sol. Cells* **2012**, *107*, 355–365.
- (14) Zhang, F.; Zang, Y.; Huang, D.; Di, C.; Zhu, D. Flexible and Self-Powered Temperature—pressure Dual-Parameter Sensors Using Microstructure-Frame-Supported Organic Thermoelectric Materials. *Nat. Commun.* **2015**, *6*, 8356.
- (15) Hattori, Y.; Falgout, L.; Lee, W.; Jung, S.-Y.; Poon, E.; Lee, J. W.; Na, I.; Geisler, A.; Sadhwani, D.; Zhang, Y.; Su, Y.; Wang, X.; Liu, Z.; Xia, J.; Cheng, H.; Webb, R. C.; Bonifas, A. P.; Won, P.; Jeong, J.-W.; Jang, K.-I.; Song, Y. M.; Nardone, B.; Nodzenski, M.; Fan, J. A.; Huang, Y.; West, D. P.; Paller, A. S.; Alam, M.; Yeo, W.-H.; Rogers, J. A. Multifunctional Skin-Like Electronics for Quantitative, Clinical Monitoring of Cutaneous Wound Healing. *Adv. Healthcare Mater.* 2014, 3, 1597–1607.
- (16) Hwang, S.-H.; Ahn, H.-J.; Yoon, J.-C.; Jang, J.-H.; Park, Y.-B. Transparent Graphene Films with a Tunable Piezoresistive Response. *J. Mater. Chem. C* **2013**, *1*, 7208.
- (17) Yamada, T.; Hayamizu, Y.; Yamamoto, Y.; Yomogida, Y.; Izadi-Najafabadi, A.; Futaba, D. N.; Hata, K. A Stretchable Carbon Nanotube Strain Sensor for Human-Motion Detection. *Nat. Nanotechnol.* **2011**, *6*, 296–301.
- (18) Li, M.; Li, H.; Zhong, W.; Zhao, Q.; Wang, D. Stretchable Conductive Polypyrrole/Polyurethane (PPy/PU) Strain Sensor with Netlike Microcracks for Human Breath Detection. ACS Appl. Mater. Interfaces 2014, 6, 1313–1319.
- (19) Wang, Y.; Wang, L.; Yang, T.; Li, X.; Zang, X.; Zhu, M.; Wang, K.; Wu, D.; Zhu, H. Wearable and Highly Sensitive Graphene Strain Sensors for Human Motion Monitoring. *Adv. Funct. Mater.* **2014**, 24, 4666–4670.
- (20) Liang, Y.; Wang, S.; Kuo, S.-W.; Wu, S.; Zhang, J.; Huang, Y.; Xiao, P.; Chen, T. Network Cracks-Based Wearable Strain Sensors for

- Subtle and Large Strain Detection of Human Motions. *J. Mater. Chem.* C 2018, 6, 5140–5147.
- (21) Yokota, T.; Inoue, Y.; Terakawa, Y.; Reeder, J.; Kaltenbrunner, M.; Ware, T.; Yang, K.; Mabuchi, K.; Murakawa, T.; Sekino, M.; Voit, W.; Sekitani, T.; Someya, T. Ultraflexible, Large-Area, Physiological Temperature Sensors for Multipoint Measurements. *Proc. Natl. Acad. Sci. U. S. A.* 2015, 112, 14533.
- (22) Sezen-Edmonds, M.; Khlyabich, P. P.; Loo, Y.-L. Tuning the Magnitude and the Polarity of the Piezoresistive Response of Polyaniline through Structural Control. ACS Appl. Mater. Interfaces 2017, 9, 12766–12772.
- (23) Lee, Y.-Y.; Lee, J.-H.; Cho, J.-Y.; Kim, N.-R.; Nam, D.-H.; Choi, I.-S.; Nam, K. T.; Joo, Y.-C. Stretching-Induced Growth of PEDOT-Rich Cores: A New Mechanism for Strain-Dependent Resistivity Change in PEDOT:PSS Films. *Adv. Funct. Mater.* **2013**, 23, 4020–4027.
- (24) Sezen-Edmonds, M.; Loo, Y.-L. Beyond Doping and Charge Balancing: How Polymer Acid Templates Impact the Properties of Conducting Polymer Complexes. *J. Phys. Chem. Lett.* **2017**, *8*, 4530–4539
- (25) Muckley, E. S.; Lynch, J.; Kumar, R.; Sumpter, B.; Ivanov, I. N. PEDOT:PSS/QCM-Based Multimodal Humidity and Pressure Sensor. Sens. Actuators, B 2016, 236, 91–98.
- (26) Herrmann, J.; Müller, K.-H.; Reda, T.; Baxter, G. R.; Raguse, B.; de Groot, G. J. J. B.; Chai, R.; Roberts, M.; Wieczorek, L. Nanoparticle Films as Sensitive Strain Gauges. *Appl. Phys. Lett.* **2007**, *91*, 183105.
- (27) Lang, U.; Naujoks, N.; Dual, J. Mechanical Characterization of PEDOT:PSS Thin Films. *Synth. Met.* **2009**, *159*, 473–479.
- (28) Pan, L.; Chortos, A.; Yu, G.; Wang, Y.; Isaacson, S.; Allen, R.; Shi, Y.; Dauskardt, R.; Bao, Z. An Ultra-Sensitive Resistive Pressure Sensor Based on Hollow-Sphere Microstructure Induced Elasticity in Conducting Polymer Film. *Nat. Commun.* **2014**, *5*, 3002.
- (29) Costa, P.; Ribeiro, S.; Lanceros-Mendez, S. Mechanical vs. Electrical Hysteresis of Carbon Nanotube/Styrene-Butadiene-Styrene Composites and Their Influence in the Electromechanical Response. *Compos. Sci. Technol.* **2015**, *109*, 1–5.
- (30) Sangeetha, N. M.; Decorde, N.; Viallet, B.; Viau, G.; Ressier, L. Nanoparticle-Based Strain Gauges Fabricated by Convective Self Assembly: Strain Sensitivity and Hysteresis with Respect to Nanoparticle Sizes. *J. Phys. Chem. C* **2013**, *117*, 1935–1940.
- (31) Segev-Bar, M.; Haick, H. Flexible Sensors Based on Nanoparticles. ACS Nano 2013, 7, 8366-8378.
- (32) Anike, J. C.; Le, H. H.; Brodeur, G. E.; Kadavan, M. M.; Abot, J. L. Piezoresistive Response of Integrated CNT Yarns under Compression and Tension: The Effect of Lateral Constraint. *J. Carbon Res.* **2017**, *3*, 14.
- (33) Chen, L.; Chen, G.; Lu, L. Piezoresistive Behavior Study on Finger-Sensing Silicone Rubber/Graphite Nanosheet Nanocomposites. *Adv. Funct. Mater.* **2007**, *17*, 898–904.
- (34) De Focatiis, D. S. A.; Hull, D.; Sánchez-Valencia, A. Roles of Prestrain and Hysteresis on Piezoresistance in Conductive Elastomers for Strain Sensor Applications. *Plast., Rubber Compos.* **2012**, *41*, 301–
- (35) Bautista-Quijano, J. R.; Avilés, F.; Aguilar, J. O.; Tapia, A. Strain Sensing Capabilities of a Piezoresistive MWCNT-Polysulfone Film. *Sens. Actuators, A* **2010**, *159*, 135–140.
- (36) Zhou, J.; Anjum, D. H.; Chen, L.; Xu, X.; Ventura, I. A.; Jiang, L.; Lubineau, G. The Temperature-Dependent Microstructure of PEDOT/PSS Films: Insights from Morphological, Mechanical and Electrical Analyses. *J. Mater. Chem. C* **2014**, *2*, 9903–9910.
- (37) Rivnay, J.; Inal, S.; Collins, B. A.; Sessolo, M.; Stavrinidou, E.; Strakosas, X.; Tassone, C.; Delongchamp, D. M.; Malliaras, G. G. Structural Control of Mixed Ionic and Electronic Transport in Conducting Polymers. *Nat. Commun.* **2016**, *7*, 11287.
- (38) Lang, U.; Muller, E.; Naujoks, N.; Dual, J. Microscopical Investigations of PEDOT:PSS Thin Films. *Adv. Funct. Mater.* **2009**, 19, 1215–1220.

- (39) Wang, H.; Ail, U.; Gabrielsson, R.; Berggren, M.; Crispin, X. Ionic Seebeck Effect in Conducting Polymers. *Adv. Energy Mater.* **2015**, *5*, 1500044.
- (40) Zhou, J.; Anjum, D. H.; Lubineau, G.; Li, E. Q.; Thoroddsen, S. T. Unraveling the Order and Disorder in Poly(3,4-Ethylenedioxythiophene)/Poly(Styrenesulfonate) Nanofilms. *Macromolecules* **2015**, *48*, 5688–5696.
- (41) Bießmann, L.; Kreuzer, L. P.; Widmann, T.; Hohn, N.; Moulin, J. F.; Müller-Buschbaum, P. Monitoring the Swelling Behavior of PEDOT:PSS Electrodes under High Humidity Conditions. ACS Appl. Mater. Interfaces 2018, 10, 9865–9872.
- (42) Kim, N.; Kee, S.; Lee, S. H.; Lee, B. H.; Kahng, Y. H.; Jo, Y. R.; Kim, B. J.; Lee, K. Highly Conductive PEDOT:PSS Nanofibrils Induced by Solution-Processed Crystallization. *Adv. Mater.* **2014**, *26*, 2268–2272.
- (43) Du, D.; Li, P.; Ouyang, J. Graphene Coated Nonwoven Fabrics as Wearable Sensors. J. Mater. Chem. C 2016, 4, 3224–3230.
- (44) Park, J. J.; Hyun, W. J.; Mun, S. C.; Park, Y. T.; Park, O. O. Highly Stretchable and Wearable Graphene Strain Sensors with Controllable Sensitivity for Human Motion Monitoring. *ACS Appl. Mater. Interfaces* **2015**, *7*, 6317–6324.